Cell Tissue Res (1985) 241:129–137

Cell and Tissue Research

Intermitochondrial junctions in the heart of the frog, *Rana esculenta*

A thin-section and freeze-fracture study

Michel Duvert[1], **Jean-Pierre Mazat**[2], **and André-Léon Barets**[1]

[1] Université de Bordeaux II, Laboratoire de Cytologie, U.A. 339 C.N.R.S., Talence, France;
[2] Université de Bordeaux II, I.B.C.N. – C.N.R.S., Bordeaux, France

Summary. In muscle fibers of the frog heart, junctions between outer membranes of adjacent mitochondrial profiles are occasionally found. In thin sections of embedded tissue and of mitochondrial pellets, the intermitochondrial junctional space is 5.4 ± 0.15 nm; the external leaflets of the membranes are joined by periodic structures separated from each other by 16.3 ± 0.29 nm. There are 65.3 ± 2 periodic structures per μm of membrane measured on a section perpendicular to the junction. After cryofracture, the outer membrane is cleaved into two parts. Closely packed, parallel rows of large particles and furrows are found either on the P-, or on the E-faces. The rows of particles are 11 ± 0.3 nm thick and are separated from each other by 16.5 ± 0.46 nm, their density being 65 ± 2.28 per μm of the membrane. In junctional areas, rows of particles on one membrane correspond with the furrows on the other membrane. Intermitochondrial junctions appear to be real structures and not artifacts due to preparation procedures. The conditions of their occurrence are discussed.

Key words: Heart – Mitochondria – Junctional structures – Cryofracture – *Rana esculenta* (Amphibia, Anura)

Intercellular junctions joining plasma membranes of adjacent cells are well known. In morphological terms, a junction can be characterized by: 1) the regularity of its extracellular space, 2) its extracellular differentiations, 3) the particular structures of the plasma membrane, and 4) the more or less obvious presence of intramembrane particles and their arrangement (Staehelin 1974; Noirot-Thimothée and Noirot 1980).

Cytoplasmic structures joining outer membranes of adjacent mitochondria have also been described in various tissues. Pease (1962) was the first to show their presence in synaptic bodies of the rod cells of cat retina, where they consisted of a strictly uniform intermembrane spacing of 12.5 nm and intermembrane bridges showing a periodicity of 16 nm. Kelly and Smith (1964) noted a similar disposition in the pineal photoreceptor cells of the frog, where mitochondria were associated in pairs. In this case, there was a pronounced beading along the directly apposing membranes of the two mitochondria, with a periodicity of about 13 nm. Fabri and Palandri (1970), and Balmefrézol and André (1970) reported similar structures in plant tissue with a much larger intermembrane spacing (35 to 40 nm). Moreover, in the latter study, purified mitochondria remained attached by this particular contact zone. Yamamoto and Kondo (1972) described "septate junctions" between adjacent mitochondria in various vertebrate tissues where the periodicity of the intermembrane bridges was 12 to 16 nm.

All these investigations were performed by use of conventional procedures, and the occurrence of intermembrane differentiations was generally described as being rare. The question therefore arises as to whether the described structures actually exist, or whether they are artifacts resulting from the preparation procedures.

In an attempt to test the influence of preparation procedures on the contact area of apposing mitochondria, we used the following techniques on the frog myocardium, where we occasionally found structures similar to those mentioned above: (i) conventional fixation of whole tissue and of mitochondrial pellets; (ii) freeze-substitution of whole tissue, according to Verna (1983); and (iii) cryofracture. This preliminary report supports the view that the structures observed in mitochondrial contact zones are real and do not result from preparative artifacts.

Materials and methods

Adult frogs, *Rana esculenta*, of both sexes were used throughout the study. After removal, hearts were immersed in Ringer solution, opened, and immobilized with a few drops of $MnCl_2$. Fixation of sino-auricular trabeculae was carried out immediately. In some experiments, hearts were incubated for 1 h in Ringer solution containing 30 mM KCN.

Some hearts were fixed according to Duvert and Barets (1979). The trabeculae were immersed, for 2 h at room temperature, in Karnovsky's fluid (Karnovsky 1965) in which the aldehyde concentration was reduced by half. After washing in 0.2 M sodium cacodylate–sodium buffer (pH 7.5), the trabeculae were transferred to a solution of 1% OsO_4 in 0.1 M sodium cacodylate – HCl buffer (pH 7.5) and left for several hours at 0–4° C. They were then washed with distilled water and stained with 1% aqueous uranyl

Send offprint requests to: M. Duvert, Laboratoire de Cytologie, Avenue des Facultés, 33405 Talence-Cedex, France

Acknowledgements. The authors would like to thank Dr. D. Gros for the cryofractures and Dr. A. Verna for Figs. 1 and 3. We thank Mrs. C. Salat for her technical assistance, Mrs. C. Fargues for typing the manuscript, and Mr. A. Heape for correcting the manuscript

acetate solution before dehydration in ethanol and embedding in Epon.

For freeze-substitution, trabeculae were dissected out and frozen on a copper block cooled by a special device (Verna 1984) to the temperature of liquid nitrogen. After freezing, the tissue was transferred to 4% OsO_4 in acetone, which had been pre-frozen in liquid nitrogen and warmed up to its melting point. The tissue was cryosubstituted in this medium for 3 days at −80° C, after which the temperature was progressively increased up to 0° C over a period of 3 h. After three brief rinses in pure acetone, the temperature was allowed to rise to room temperature and the specimen was embedded in Araldite. After polymerization, thin sections were cut and contrasted as usual.

Heart mitochondria were prepared as follows, at 1° C: six frog hearts were washed in cold M.S.E. medium (0.0225 M mannitol, 0.075 M sucrose, 0.05 mM EGTA and 20 mM Tris maleate, pH 7.2), and finely chopped with a pair of scissors. The fragments were rapidly homogenized with a glass homogenizer (30–60 s) and the homogenate was immediately centrifuged at 8000 g for 10 mn. The pellet was resuspended in M.S.E. medium. After a second centrifugation at 700 g for 10 min the supernatant was centrifuged 8000 g for 10 min and the resulting pellet was fixed in half-strength Karnovsky's fluid (Duvert and Barets 1979) for 1 h at 0–4° C, or at room temperature. Some of the pellets were then immersed directly in 1% OsO_4 in a 0.1 M sodium cacodylate buffer solution containing 73.5 mg % $CaCl_2$ and 2% PVP, and left for several hours at 0–4° C, while others were prewashed in 0.2 M sodium cacodylate – HCl buffer for 1 h at room temperature. They were then washed five times for 10 min in distilled water, followed by a 30 min immersion in 1% aqueous uranyl acetate. The pellets were rewashed, dehydrated and embedded in Epon. In one experiment, the sample was treated with 1% tannic acid in 0.05 M sodium cacodylate buffer (pH 7.2), for 1 h at room temperature, between the OsO_4 postfixation and treatment with uranyl acetate. In a few experiments, hearts were treated with Nagarse before homogenization, as described by Tyler and Gonze (1967).

For cryofracture, hearts were immersed in a 3.5% glutaraldehyde solution in 0.067 M sodium cacodylate buffer (pH 7), containing 1 mM $CaCl_2$ and 0.6% glucose, for 1 h at room temperature. Small trabeculae were cut out and transferred sequentially into 10, 20 and 30% glycerol solutions in 0.1 M sodium cacodylate buffer (pH 7.2). They were then mounted on gold disks and frozen in Freon 22 that had been pre-cooled with liquid nitrogen. Freeze-fracturing at −100° C and platinum-carbon replicas were carried out using a Balzers apparatus equipped with electron guns.

Sections were stained with uranyl acetate and lead citrate as usual. Sections and replicas were observed in a Philips EM 300 electron microscope. Magnifications were calibrated with the use of a cross-grating replica (2160 lines/mm), and fracture faces were named according to the nomenclature of Branton et al. (1975).

The sizes of intramembrane particles and pits were measured from prints (final magnifications: ×60000) in the direction of the shadowing with a Leitz micrometer eyepiece (1 cm divided into 0.1 mm sections). Diameters were measured only on relatively flat surfaces and not in membrane regions presenting curves.

For the determination of particle and pit densities, the print was enlarged (final magnification: ×150000) and a square lattice, with each square representing 1 μm^2, was placed at random on the relatively flat surfaces, again excluding curved membrane regions. The number of particles and pits in the squares was counted.

In thin sections, the intermembrane spaces were measured at perpendicular sections, in which the two mitochondrial membranes, with their two leaflets, were clearly defined. Only strictly perpendicular sections, or very nearly perpendicular sections, were used for measuring the periodicity of the junctional structures.

Unless otherwise stated, the results are expressed as the mean of n measures (n given in brackets), with its standard deviation.

Results

I. Thin sections

A) Whole tissue

Conventional fixation. In some cases, closely apposed mitochondria can be seen. In the apposition zone (Fig. 1), periodic structures (16 to 18 nm periodicity, Fig. 25) bridge the

Figs. 1–4. Thin sections of fibers

Fig. 1. Close contact between two mitochondria; *arrow* shows periodic structures bridging the gap between the apposed membranes; ×91200

Fig. 2. Detail of the periodic structures: each one seems to be composed of two parts; ×188000

Fig. 3. Longitudinal section of a freeze-substituted fiber; note some ramified mitochondria with a dense matrix; ×18200

Fig. 4. Oblique section in close contact zones between mitochondria in a freeze-substituted tissue. Note the parallel rows (*arrowhead*); ×89400

Figs. 5–8. Thin sections of mitochondrial pellets

Fig. 5. Profiles of adjacent mitochondria are linked by junctions (*arrows*), and one mitochondrial section can be linked to various other mitochondrial profiles; ×58800

Figs. 6, 7. High magnification showing the periodic structures crossing the intermembrane space. Fig. 6: ×144000, Fig. 7: ×190000

Fig. 8. Fixative containing tannic acid; the periodic structures are no longer visible (*arrows*): ×75600

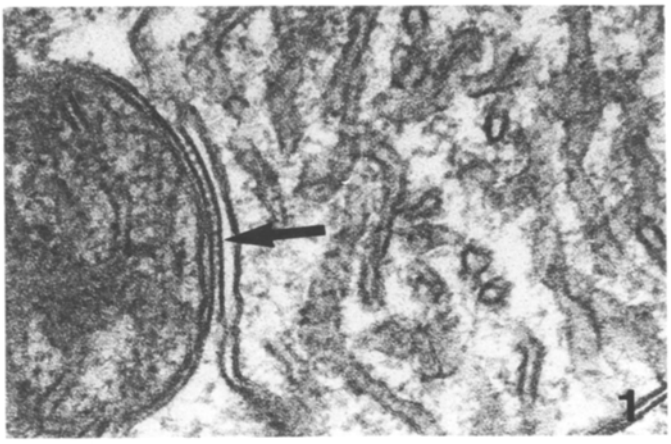
1

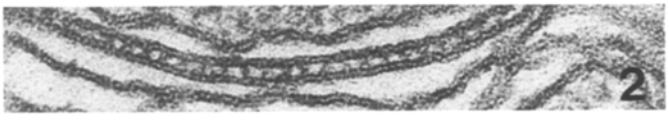
2

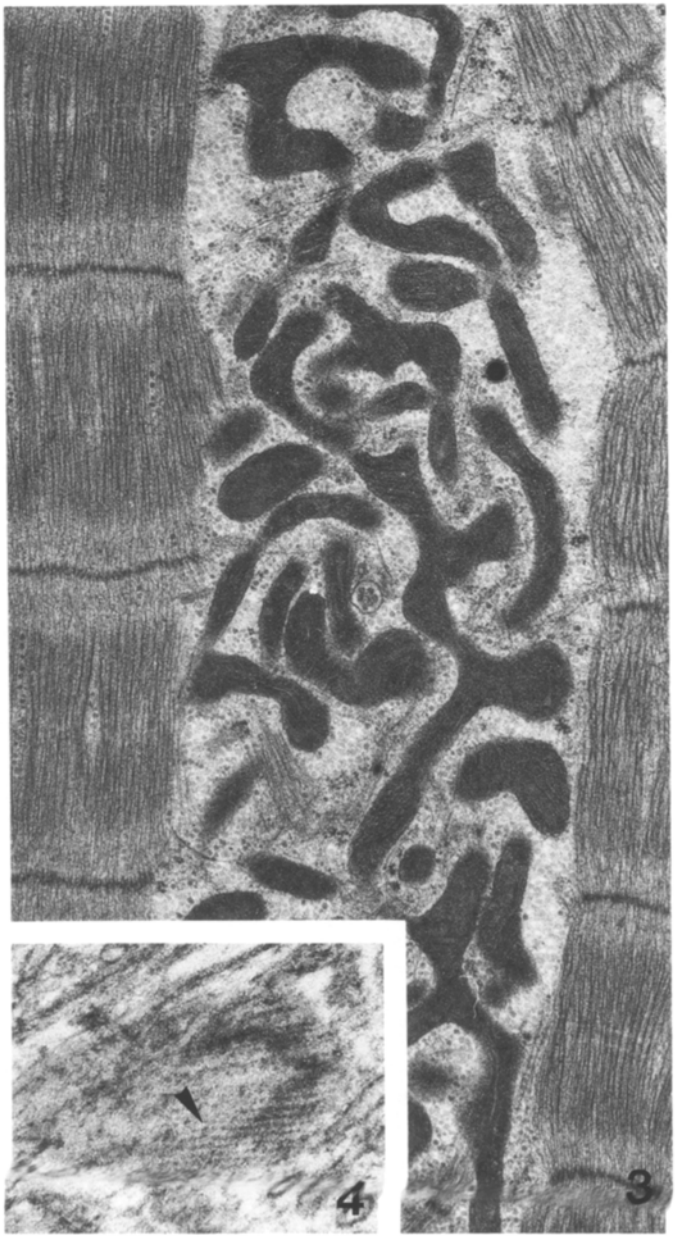
3

4

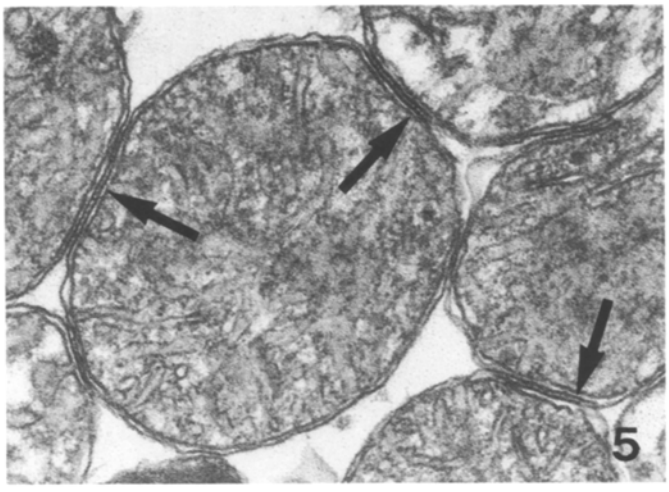
5

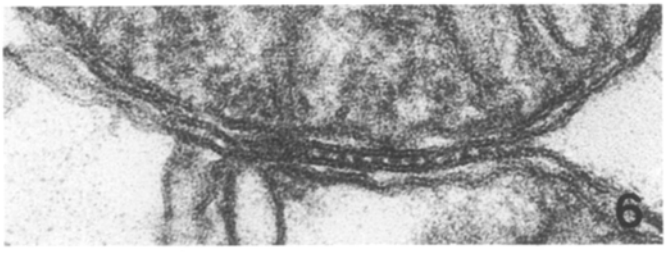
6


7

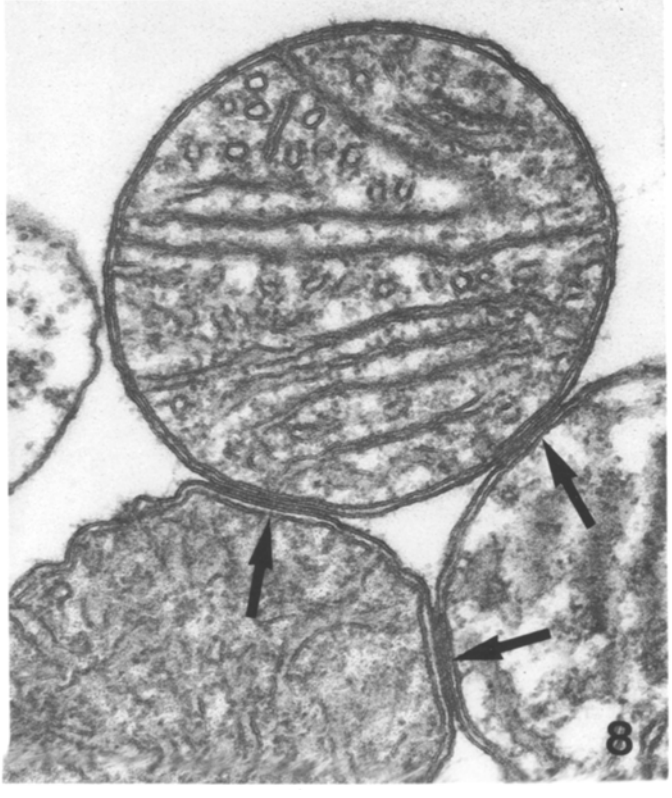
8

6 to 7 nm gap between the outer membranes (Fig. 23). These periodic structures linking the membranes appear to consist of two components that meet in the center of the junction (Fig. 2), and they have no apparent relationship with the inner membrane. Moreover, these junctions seem to be more abundant when hearts are incubated for 1 h in Ringer solution containing 30 mM KCN (Fig. 2).

Freeze-substitution. Mitochondria have a long and ramified appearance; the intermembrane space is very reduced, the intracristae spaces are not always visible (Fig. 3), and the matrix is highly electron dense. In oblique sections, parallel rows of what seem to be punctate structures can be seen between two adjacent mitochondria (Fig. 4). The distance between two such rows is about 15 nm.

B) Mitochondrial fractions

Junctions are frequently observed in the mitochondrial fractions, thus permitting numerous measurements to be made (Figs. 5–7). The gap between the outer membrane faces is 5.4 ± 0.15 nm ($n=41$). Periodic structures, with a periodicity of 16.3 ± 0.29 nm ($n=61$), are numerous (63.34 ± 2.01 μm of junctional membrane, Fig. 24) and are only related to the outer membranes. Electron-dense markers, such as tannic acid-lead, do not allow a clear visualization of the junctional structures (Fig. 8).

II. Cryofractures

A) The inner membranes. The concave faces, or EF (Fig. 10), reveal a network of thick particles, 14 ± 0.7 nm ($n=31$) in diameter, with a density of about $1700/\mu m^2$ (this is only an indication, since very few EF are observed), and protrusions (about 45 nm in diameter) that may support the cristae.

The convex face, or PF (Fig. 11), contains depressions and 3270 ± 185 particles/μm^2 ($n=5$); these particles have a diameter of 11.6 ± 0.29 nm ($n=155$).

Inner membrane faces are rare (about 5% of the mitochondrial outer plus inner membrane faces). The matrix and crests are not studied in this work.

B) The non-junctional outer membranes. The outer membranes represent at least 95% of the fracture faces (Fig. 9). One half consists of the concave faces, while the other half consists of the convex faces.

On the concave P-faces (Fig. 12), two groups of particles are arranged in a network and are intercalated by irregularly shaped, smooth areas of about 25×75 nm. The large particles are polyhedral or lozenge-shaped and have a low relief; they seem to rise slowly and to stop abruptly at the level of a short white margin. Their dimensions are $15 \pm 0.24 \times 19.9 \pm 0.33$ nm ($n=169$). The small particles have a sharp relief and their diameter is 7.2 ± 0.19 nm ($n=82$). The membrane particle density is $2416 \pm 125/\mu m^2$ ($n=12$). Some pits (6 to 10 nm in diameter, mean = 9 nm) are found near the particles.

The convex E-faces (Fig. 13) are characterized by small pits 9.7 ± 0.1 nm in diameter ($n=298$), arranged in a network. This network lines smooth areas of about 10×80 nm. A strong similarity is apparent in some micrographs between the networks of particles and pits on the two types of faces (Figs. 9, 12, 13). Large polyhedral particles, like those already described on the concave faces, can be seen near some pits. Their dimensions are $12.7 \pm 0.6 \times 16.6 \pm 0.7$ nm ($n=24$). The intramembrane particle density is $2200 \pm 159/\mu m^2$ ($n=9$).

C) The junctional portion of the outer membranes. On the E-face, there are either parallel rows of particles (Figs. 14, 15), or parallel rows of pits fused in furrows (Fig. 16). Parallel rows of particles with a high relief (Fig. 17) and rows of furrows are also observed on the P-face; the mean thickness of a row of particles is 11 ± 0.3 nm ($n=27$). The mean distance between two rows of particles, or between two rows of pits, is 16.5 ± 0.46 nm ($n=74$) (Fig. 24). In a plane perpendicular to the rows and to the membrane, 65.8 ± 2.28 rows of particles can be found along 1 μm of membrane ($n=12$) (Fig. 25). While a strong cohesion between particles in a single row is apparent, adjoining rows do not seem to be so closely related. In fact, groups of rows can be divergent. Within the rows, the particles are polyhedral and their apex at the fracture face level is not smooth, suggesting a depression.

When two mitochondria are in close apposition, the rows of particles correspond in the two membranes (Figs. 19–22). Fig. 20 shows three fracture faces of mitochondria (two concave faces and a convex one). On the right of the concave face, rows of particles correspond to

Figs. 9–25. Cryofractures. (Direction of shadowing from the bottom to the top of the micrographs)

Fig. 9. E- and P-faces of outer mitochondrial membranes; note the ridge delimiting the convex faces and the cytoplasm (*arrows*); × 56800

Fig. 10. Concave face of an inner membrane covering the P-face of an outer membrane; note the protrusions (*arrow*); × 93600

Fig. 11. Convex face of an inner membrane with depressions (*arrow*); × 90700

Fig. 12. P-face of an outer membrane; on the left, the fracture crosses the matrix and crests. On the P-face, there is a network of large polyhedral particles with a low relief; some small particles with a high relief can be seen (*arrows*); × 126000

Fig. 13. E-face of an outer mitochondrial membrane. A network of pits is clearly visible with some rare polyhedral particles. Note the ridge next to the cytoplasm (*arrow*); × 117600

Fig. 14. E-face of an outer membrane showing parallel rows of particles (between the two *arrows*); × 106200

Fig. 15. E-face of an outer membrane; several parallel rows of particles, apparently with a central depression, can be seen; × 222700

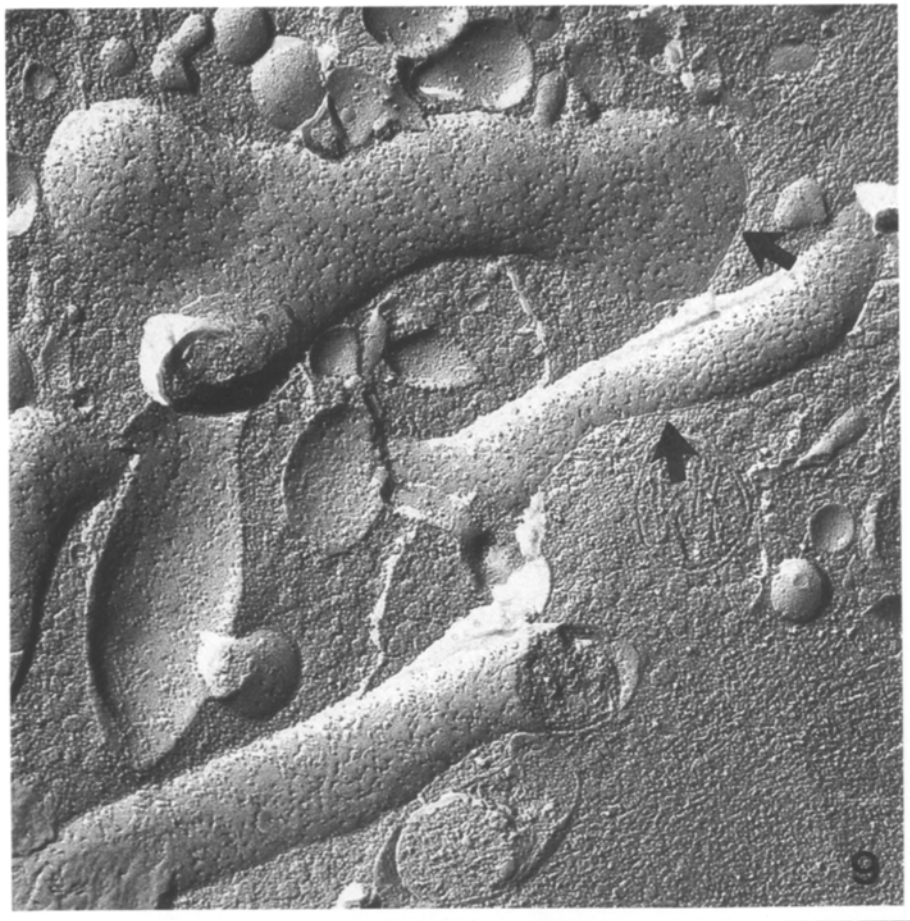
9

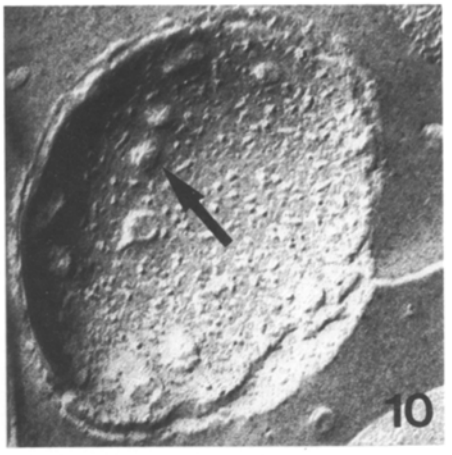
10

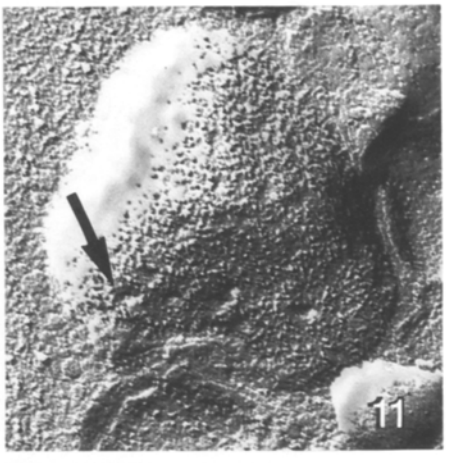
11


12

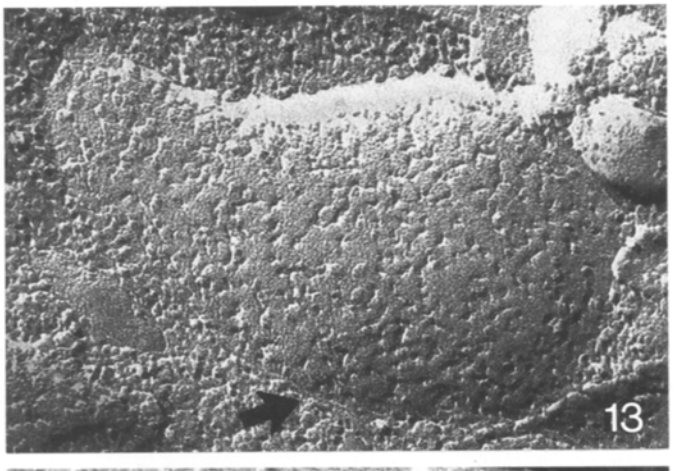
13

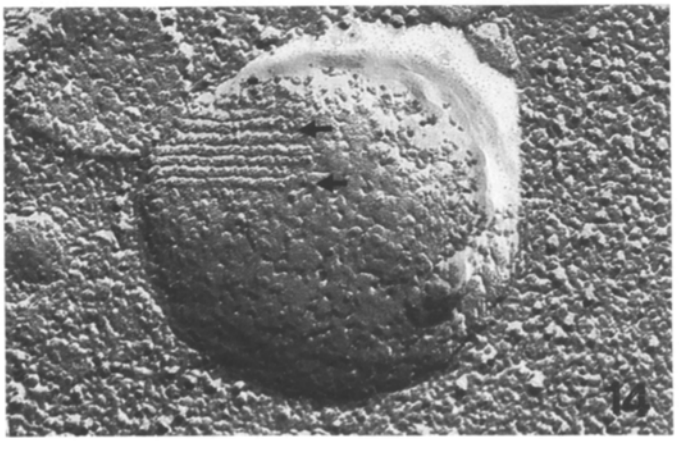
14

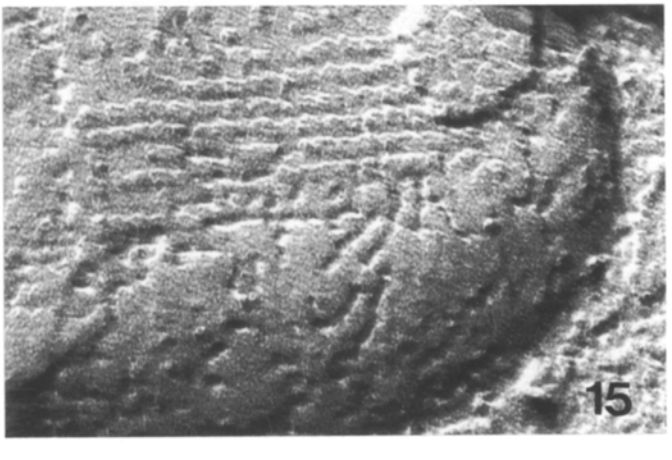
15

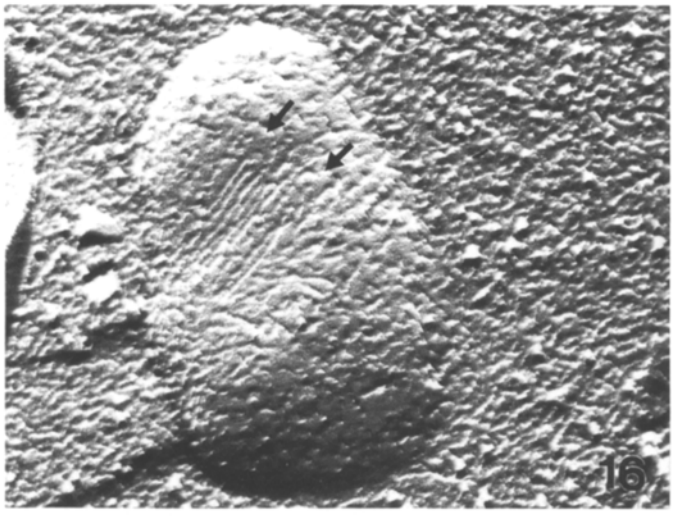
16


17


18

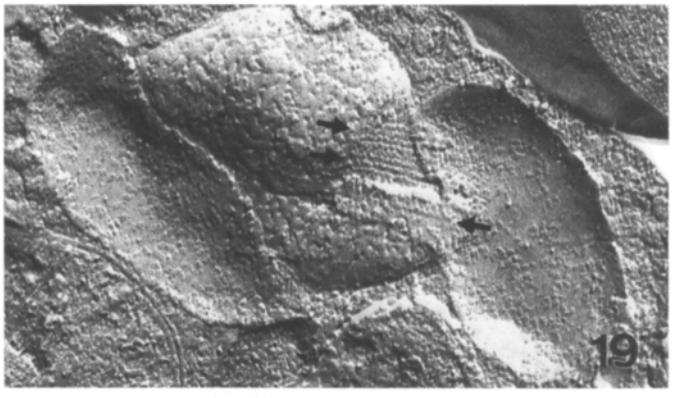
19

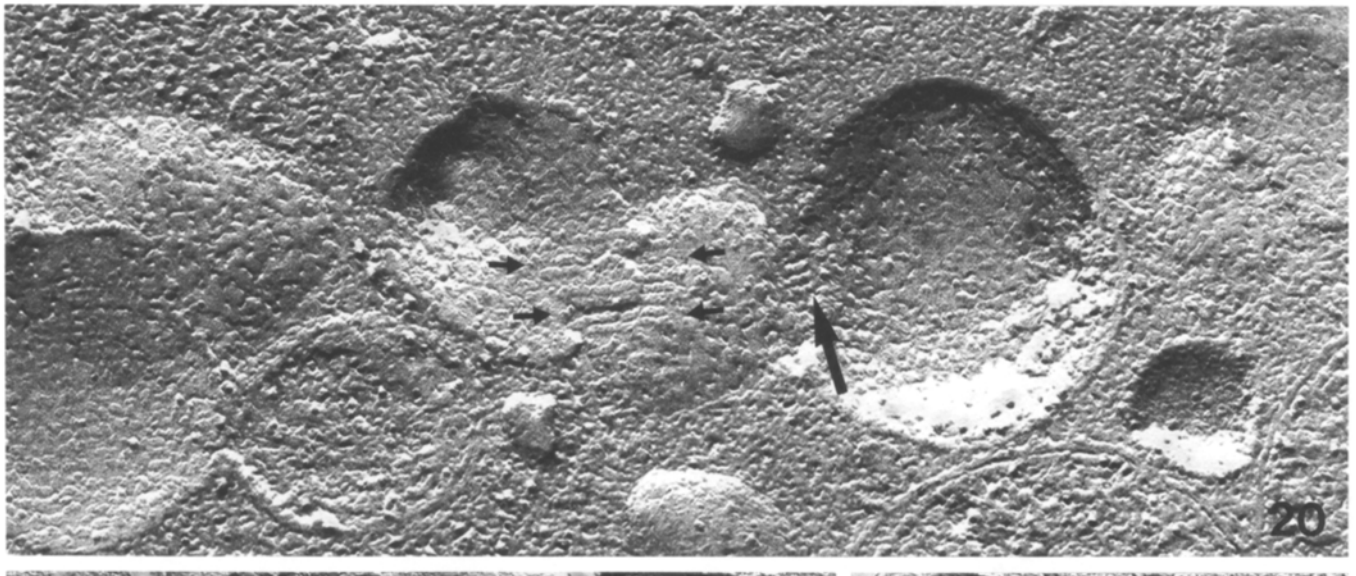
20


21

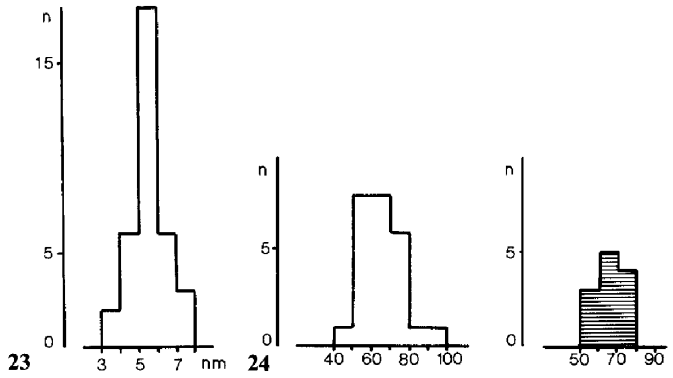

Fig. 23. Intermembrane space (nm) as a function of the number of junctions measured, $n=35$

Fig. 24. Number of junctional structures per μm of junctional membrane: thin sections (*left*) $n=48$, freeze-fracture (*right*) $n=71$

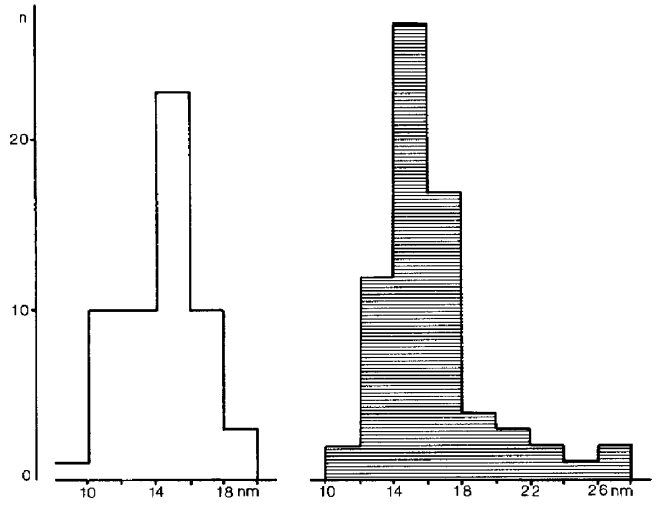

Fig. 25. Periodicity of junctional structures: thin section (*left*) $n=25$, freeze-fracture (*right*) $n=12$

the contiguous rows of particles on the convex face; these structures are constituted by parallel rows of particles that correspond exactly in the two membranes. Fig. 18 shows the correspondence between intramembrane rows of particles and cytoplasmic periodic structures.

Large zones of apposition are not frequently observed. However, segments of such appositions (Figs. 21, 22), where parts of parallel rows of particles or furrows may occur in small areas, can often be found. In all these cases, the images suggest the correspondance of rows in the two membranes.

Discussion

The various techniques used in this investigation give coherent results concerning the structures found in some specialized contact zones of adjacent mitochondria:

(1) The intermembrane spaces, measured in sections of whole tissue (after conventional fixation or after freeze-substitution) and in sections of mitochondrial pellets (after conventional fixation), are regular and of similar appearance. (2) Structures bridging outer membranes of adjacent mitochondria are seen not only after preparation procedures of whole tissue, but also in mitochondrial pellets. They show the same periodicity in both cases. (3) Morphological data concerning these contact zones are comparable to those reported in the literature for these specialized regions in other tissues of various animals. (4) Most importantly, cryofractures constantly show regular arrangements of intramembrane particles in specialized contact zones. Their periodicity corresponds to that of the bridging structures.

Hence, using the same approach that enabled the definition of plasma membrane junctions (Staehelin 1974; Noirot Timothée and Noirot 1980), we conclude that the contact zones observed here probably represent real junctions, which we call intermitochondrial junctions (IMJ). In fact, we are unable to demonstrate whether IMJ link two individual mitochondria, or different parts of a single mitochondria. Micrographs of freeze-substituted cells of frog myocardium show many large and ramified mitochondria. The three-dimensional arrangement of these organelles is complex and various sections of the same mitochondria may arise on a micrograph. Cryofracture data present certainly the most important arguments in favour of the reality of IMJ and, for this reason, they deserve further comment. We shall successively examine the fracture faces, the intramembrane particles and, finally, the junctional areas.

The fracture faces. In their study of heart mitochondrial membranes, Sjöstrand and Cassell (1978) claimed that outer mitochondrial membranes show their true faces on replicas. We do not agree with this interpretation regarding the frog heart mitochondria. According to Branton et al. (1975) and various other authors (Hackenbrock 1972a; Packer 1972, 1973, 1974), the fracture plane of the outer membrane is

Fig. 16. E-face of an outer membrane showing parallel furrows (between the two *arrows*); ×81400

Fig. 17. P-face of an outer mitochondrial membrane. *Arrows* show parallel ridges of particles; ×164000

Fig. 18. Two mitochondria are in close contact. On the left, the outer membrane is cleaved and shows an E-face with rows of particles. On the right, the fracture traverses a mitochondrium. Rows of particles are continuous with cytoplasmic structures joining the membranes (*arrow*); ×67900

Fig. 19. Two outer mitochondrial membranes overlap (*arrows*). In this junctional area, parallel rows of particles are seen in the two membranes (EF on the left, PF on the right); ×67900

Fig. 20. Fracture through three outer mitochondrial membranes; two P-faces lie against a central E-face. In the junctional area, rows of particles on two membranes are in co-alignment (*small arrows*). *Large arrow* indicates another possible junctional zone; ×106200

Figs. 21, 22. Portions of mitochondrial junctions (*arrows*); Fig. 21: ×38100; Fig. 22: ×58800

intramembranous. This interpretation is supported by four results:

(1) Convex faces (EF) can be separated from cytoplasm by a ridge, which may represent part of the cleaved membrane. (2) The particles on the P-face are arranged in a network, like the pits on the E face, and they line smooth patches. The networks and the patches are of comparable size on both E- and P-faces. (3) The particle density on the P-face corresponds to the density of the pits on the E-face. (4) There is a complementarity between the E- and P-faces, despite the fact that the dimensions of the large particles on the latter do not correspond to the diameters of the pits, which are smaller, on the E-face. This is often the case in replicas (Bullivant 1973).

Regarding the above observations, it is our opinion that outer membrane E and P-faces are complementary, and that the freeze-fracture crosses this membrane. Consequently, the rows of particles and furrows seen in junctional regions are true intramembrane structures.

Intramembrane particles. Intramembrane particles seen in outer mitochondrial membranes have variable dimensions, comparable to values found by Sjöstrand and Cassell (1978) in outer mitochondrial membranes of the rat heart. Moreover, according to other observations in various tissues (Melnick and Packer 1971; Hackenbrock 1972a; Packer 1972; Ashraf 1978), they are preferentially localized on the P-face. According to Sjöstrand and Cassell (1978), two kinds of particles are observed in these membranes; their morphology appears to be comparable in the frog and rat hearts, but the mean size of the smallest particles is somewhat different in the two species.

In mitochondrial membranes, particles are arranged in a network, some characteristics of which may vary as a result of preparatory procedures, or of the metabolic state of the mitochondria (Wrigglesworth et al. 1970; Höchli and Hackenbrock 1976). The particles could represent parts of protein or lipoprotein molecules, while the smooth areas lined by the particles could represent lipidic regions (Packer 1974; Höchli and Hackenbrock 1976). The particle density reported in the outer mitochondrial membranes of the frog heart is very similar to that reported by Packer (1972) in liver mitochondria, but higher than that found by Ashraf (1978) in dog-heart mitochondria. The dimensions of the smooth areas are comparable to those reported by Hackenbrock (1972a). In structural terms, therefore, it would seem that the outer mitochondrial membranes of frog-heart fibers do not differ substantially from other mitochondrial outer membranes described in the literature.

The junctional areas. In the junction described in this paper, parallel rows of intramembrane particles are clearly visible owing to their high relief and their strong lateral cohesion within rows. The density of the rows and their periodicity correspond to the density and the periodicity of the structures joining the membranes in thin sections (Figs. 24, 25). These structural relationships strongly suggest that the structures seen on thin sections are linked to the rows of intramembrane particles in a way that remains to be investigated; a morphological relationship between intramembrane particles and extra-membrane structures can be seen in Fig. 18.

The junctional particles showed strong lateral cohesion within rows, but, under the experimental conditions of this study, they did not have a preferential affinity for E- or P-faces. It must be underlined that groups of rows are either on P-faces, or on E-faces; these observations suggest some kind of lateral but weak cohesion between neighbouring parallel rows. Further studies are needed to verify these data since glutaraldehyde and glycerol were used in this work. It is known that, at low concentrations, and over brief times of action, these substances preserve the mitochondrial membrane architecture, but may alter their particle morphology and distribution (Wrigglesworth et al. 1970; Hackenbrock 1972b; Sjöstrand and Bernhard 1976). Moreover, other factors, such as pH, temperature and hydratation, strongly affect the distribution of particles (Packer 1972; Höchli and Hackenbrock 1976). These conditions were kept constant under our experimental procedures, and their effects were, therefore, probably minimized.

It is not easy to compare intermitochondrial junctions with intercellular junctions since the intermembrane space is intracellular instead of intercellular. Any resemblance with invertebrate septate junctions is meaningless.

Are intermitochondrial junctions permanent or transitory structures? Some data indicate that their occurrence is related to particular physiological conditions. Bulger and Trump (1968) reported regular septa between apposed mitochondria in degenerating cells, or in cells deprived of an energetic source, in rat and flounder renal tubules; they do not occur in normal cells. Watanabe et al. (1976) described septate-like junctions between mitochondria of adrenal chromaffine cells in human phaeochromocytoma, in association with a reduction in the activity of mitochondrial enzymes. These structures are not seen in normal tissue. Harris (1979) reported a similar junction in fat body cells of the pre-hatch larvae of an insect; this structure may develop in order to improve metabolic efficiency after stress. Verna and Duvert (1984) showed that in sensory cells of the carotid body of the rabbit, and in sino-atrial cells of the frog, cyanide increases the occurrence of intermitochondrial junctions in vivo and in vitro. Hence, it may be concluded that intermitochondrial junctions could be transitory structures and that their occurrence could be related to the activity of the respiratory chain in a way that remains to be defined. Their significance is unknown and has to be viewed within the new concept of mitochondria as highly flexible structures interacting extensively with other cellular structures, including other mitochondria (Yaffe and Schatz 1984).

References

Ashraf M (1978) Ultrastructural alterations in the mitochondrial membranes of ischemic myocardium as revealed by freeze-fracture technique. J Mol Cell Cardiol 10:535–543

Balmefrézol M, André J (1970) Observation d'un mode inhabituel d'association de mitochondries. Septième congrès Mic Electr Grenoble, 125–126

Branton D, Bullivant S, Gilula NB, Karnovsky MJ, Moor H, Mullethaler K, Norhcote DH, Packer L, Satir B, Satir P, Speth V, Staehelin LA, Steer RL, Weinstein RS (1975) Freeze-etching nomenclature. Science 190:54–56

Bulger RE, Trump BF (1968) Occurrence of repeating septate subunits between apposed cellular membranes. Exp Cell Res 51:587–594

Bullivant S (1973) Freeze-etching and freeze-fracturing. Advances in biological electron microscopy. Springer, Berlin, Heidelberg, New York, pp 67–112

Duvert M, Barets A (1979) Fine structure and organization of the sarcoplasmic reticulum in the sino-auricular fibers of the frog. Z Naturforsch 34c:865–875

Fabri F, Palandri M (1970) Mitocondri aggregati in *Psilotum nudum* (L.). Caryologia 23:441–453

Hackenbrock CR (1972a) States of activity and structure in mitochondrial membranes. Ann New York Acad Sci 195:492–505

Hackenbrock CR (1972b) Energy-linked ultrastructural transformations in isolated mitochondria and mitoplasts. Preservation of configurations by freeze-cleaving compared to chemical fixation. J Cell Biol 53:450–465

Harris DF (1979) Intermitochondrial bridge junctions in fat body cells of the pre-hatch larvae of the forest tent caterpillar *Malcosoma disstria*. HBN Eur J Cell Biol 19:131–134

Höchli M, Hackenbrock CR (1976) Fluidity in mitochondrial membranes: thermotropic lateral translational motion of intramembrane particles. Proc Natl Acad Sci USA 73:1636–1640

Karnovsky JM (1965) A formaldehyde-glutaraldehyde fixative of high osmolality for use in electron microscopy. J Cell Biol 27:137A

Kelly DE, Smith SW (1964) Fine structure of the pineal organs of the adult frog, *Rana pipiens*. J Cell Biol 22:653–674

Melnick RL, Packer L (1971) Freeze-fracture of inner and outer membranes of mitochondria. Biochim Biophys Acta 253: 503–508

Noirot-Timothée C, Noirot C (1980) Septate and scalariform junctions in arthropods. Int Rev Cytol 63:97–140

Packer L (1972) Functional organization of intramembrane particles of mitochondrial inner membranes. Bioenergenic 3: 115–127

Packer L (1973) Membrane particles of mitochondria. Mechanisms in bioenergetics. Academic Press New York, San Francisco, London, pp 32–52

Packer L (1974) Molecular architecture of energy transducing membranes related to function. Biomembranes. Architecture, biogenesis, bioenergetics and differentiation. Academic Press New York, San Francisco, London, pp 147–166

Pease DC (1962) Demonstration of a highly ordered pattern upon a mitochondrial surface. J Cell Biol 15:385–389

Sjöstrand FS, Bernhard W (1976) The structure of mitochondrial membranes in frozen sections. J Ultrastruct Res 56:233–246

Sjöstrand FS, Cassel RZ (1978) The structure of the surface membranes in rat heart muscle mitochondria as revealed by freeze-fracturing. J Ultrastruct Res 63:138–154

Staehelin LA (1974) Structure and function of intercellular junctions. Int Rev Cytol 39:191–283

Tyler DD, Gonze J (1967) The preparation of heart mitochondria from laboratory animals. In: RW Estabrook, ME Pullman (ed) Methods in enzymology, Academic Press New York, London, X, 75–77

Verna A (1983) A simple quick-freezing device for ultrastructure preservation: evaluation by freeze-substitution. Biol Cell 49:95–98

Verna A, Duvert M (1984) Formation de jonctions entre mitochondries après administration de cyanure in vivo et in vitro. Biol Cell 51:14a

Watanabe H, Burnstock G, Jarrott B, Louis WJ (1976) Mitochondrial abnormalities in human phaeochromocytoma. Cell Tissue Res 172:281–288

Wrigglesworth JM, Packer L, Branton D (1970) Organization of mitochondrial structure as revealed by freeze-etching. Biochim Biophys Acta 205:125–135

Yaffe M, Schatz G (1984) The future of mitochondrial research. Trends Biochem Sci 9:179–181

Yamamoto, TY, Kondo H (1972) Occurrence of septate junctions between adjacent mitochondria. Acta Histochem Cytochem 5:263–265

Accepted February 18, 1985